Incorporation of Nascent Myosin Heavy Chains into Thick Filaments of Cardiac Myocytes in Thyroid-treated Rabbits

Mary P. Wenderoth and Brenda R. Eisenberg

Department of Physiology, Rush Medical College, Chicago, Illinois 60612

Abstract. A monoclonal antibody (mAb 37) specific for α-myosin heavy chain (α-MHC) is used to follow the spatial and temporal incorporation of α-MHC into rabbit left ventricular myocytes. The expression of the two adult cardiac MHC genes, α and β, is regulated by manipulating the thyroid hormone level of the animal. 10 wk on a propylthiouracil diet down-regulates expression of α-MHC to near 0%. α-MHC gene expression is up-regulated by injecting L-triiodothyronine (100 μg/kg per d) for 1–4 d. This protocol provides a means by which to follow the redistribution pattern of α-MHC within the myocyte in vivo. A uniform distribution of immunofluorescent signal is seen within every myocyte throughout the left ventricle. Ultracryomicrotomy without fixation is used to obtain sections for immunogold-electron microscopy. To quantify the immunogold method the density of gold-labeled antibody per unit of area tissue is determined for various regions of the sarcomere. Tissue from normal and 2-wk baby has a uniform distribution of gold density along the length of the A band. The average gold density of the A band increases with days of thyroid injection from 38 ± 4 grains/μm² (n = 2 animals) (mean ± SE) at day 1 to 182 ± 59 grains (n = 2 animals) at day 4. There is a nonuniform incorporation of the newly synthesized α-MHC within the A band of thyroid-treated animals since 50% more of the α-MHC is found at the end of the A band while the center of the A band has 40% less than the average α-MHC content (grains/μm², n = 7 animals). These results support a thick filament assembly model that allows every myosin in a thick filament to be exchanged with new myosin. However, in the intact functioning myocyte, there is greater exchange of new myosin at the ends than in the central region of the thick filament.

THE thick filament of muscle is composed of approximately 300 myosin molecules whose function is to generate force during muscle contraction. Cardiac myosin is degraded and replaced with a half life of 8 d in the rabbit (Morkin et al., 1972) and the turnover process is accomplished without interrupting the force-generating function of the muscle fiber. Because of this special constraint, the nature of thick filament assembly and the mechanism involved with exchange of myosin within that filament have long been areas of scientific inquiry.

Huxley (1963) showed that free myosin molecules could spontaneously form thick filaments when the ionic strength of the solution was lowered. Further work on the self-assembly process revealed that strong ionic interactions exist between the rod regions of myosin molecules and are responsible for spontaneous assembly (for review see Harrington and Rodgers, 1984). In an attempt to understand the mechanisms that may regulate thick filament assembly, numerous investigators have studied the system in vitro by varying pH, ionic strength (for review see Pepe, 1983; Harrington and Rodgers, 1984), temperature, calcium concentration (Higuchi and Ishiwata, 1985), and in the presence of sodium pyrophosphate (Reisler et al., 1986). Saad et al. (1986*a*, *c*) studied the rapid kinetics of thick filament assembly with the fluorescence energy transfer system and found that a monomeric pool of myosin is in a state of dynamic exchange with thick filaments. However, synthetic thick filaments lack many of the structural and functional elements of the living muscle fiber that might alter both the kinetics of the assembly process and the size of the free myosin pool.

One reason why myosin exchange has not been studied in vivo is the difficulty in localizing newly synthesized myosin within the muscle fiber. In the past the only method available was by autoradiographic analysis of tissue that had been infused with radioactive amino acid precursors. Unfortunately, this method labels all new proteins nonspecifically and can not identify the cellular distribution of myosin alone.

The design of the present experiment takes advantage of the fact that cardiac myosin heavy chain (MHC)[1] exists in two isoforms, α and β, and the expression of the isoforms can be regulated by manipulating the thyroid level of the animal. Investigations have shown that the level of α-MHC expression can be completely down-regulated by inducing a state of hypothyroidism in the experimental animal (Hoh et al., 1978). We found that 10 wk at a low plasma thyroid level

1. *Abbreviations used in this paper*: GAr, goat anti-rat; MHC, myosin heavy chain; PTU, propylthiouracil.

(100 ng/dl) was needed to switch off the α-MHC gene for a sufficient period of time to ensure that all preexisting α-MHC protein was removed. Up-regulation of α-MHC gene is accomplished by increasing the plasma thyroid level (Chizzonite et al., 1982) with injections of L-triiodothyronine.

A second aspect that is critical to the design of this study is the availability of a method to differentiate between the α and β isoforms of MHC. Even though the isoforms share 95% homology of amino acid sequence (Umeda et al., 1986), a monoclonal antibody, mAb 37, specific for the α-MHC isoform has been developed (Chizzonite et al., 1982). The sites of incorporation of α-MHC into the thick filament are monitored by immunogold-electron microscopy.

There are many possible patterns of incorporation of new myosin into thick filaments. One pattern would be de novo synthesis of new filaments to replace old. Another is a random incorporation of new myosin along the length of the filament. A third is preferential addition of new myosin at some site along the thick filament. Our results show that during the period of induced isomyosin switching nascent myosin is incorporated throughout the length of the thick filament. However, a preferential addition of the nascent myosin to the ends of the thick filament is also observed.

Materials and Methods

Thyroid Model and Tissue Preparation

10 New Zealand White rabbits (2.0–3.0 kg) were placed on a propylthiouracil (PTU)-enriched diet (Teklad Diets, Madison, WI) for 70 d to induce hypothyroidism (Everett et al., 1984). At the end of this time the rabbits were injected intraperitoneally with L-triiodothyronine (L-T3; Sigma Chemical Co., St. Louis, MO) in saline solution (1 mg/ml) at a dose level of 100 μg/kg per d for 1–4 d. The animals were killed by the infusion of a high potassium solution (Kovacs et al., 1983) into the vena cava to depolarize the heart and produce a state of relaxation. The heart was removed, the ventricles dissected, blotted dry, and weighed. The papillary muscles of the left ventricle were dissected free from the heart wall and pinned down at rest length to prevent contraction during subsequent dissection and sucrose infiltration.

Immunofluorescence

Procedures for indirect immunofluorescence were as presented in previous work (Eisenberg et al., 1985). Frozen sections were incubated in mAb 37 diluted 1:100 (a gift from Dr. R. Zak, University of Chicago, Chicago, IL), and in rabbit anti-rat IgG FITC at a 1:100 dilution, (CooperBiomedical, Inc., Malvern, PA) and viewed with a Nikon epifluorescent microscope. Controls consisted of omission of the primary antibody, mAb 37; omission of the secondary antibody, rabbit anti-rat IgG FITC; omission of both antibodies; and replacement of mAb 37 with rat serum as a positive control.

Specificity of mAb 37 for α-MHC has been previously confirmed by Zak et al. (1982) using competitive RIA. Eisenberg et al. (1985) used the technique of rotary shadowing of the myosin-antibody complexes to localize the site of antibody binding to the hinge region of the tail of the myosin molecule.

Ultracryomicrotomy

The methods of Tokuyasu (1986) were followed for both ultracryomicrotomy and immunostaining. Small blocks of tissue from the papillary muscles were immediately cryoprotected with 2.3 M sucrose in 0.1 M PBS. The antibody, mAb 37, no longer bound to the antigenic site after the following fixations: 0.2% glutaraldehyde (perfused or immersed); 3% paraformaldehyde; paraformaldehyde/lysine/sodium m-periodate (PLP fixation) (McLean and Nakane, 1974); 3% paraformaldehyde and 20 mM ethylacetimidate (Tokuyasu et al., 1981); 0.35% glutaraldehyde, 1.4% Tris, 50% PBS, 1% ethyl-3(dimethylaminopropyl)carbodiimide (Willingham and Yamada, 1979), and dimethylsuberimidate (20 mg/ml) (Kuettel et al., 1985); and parabenzoquinone in 0.1 M PBS (Pearse and Polak, 1975). Although antigenicity was maintained with acetone/methanol fixation, the plasticity of the frozen block was incompatible with ultracryosectioning. Therefore, no form of fixation was used before cryoprotection and the ionic strength of all solutions were maintained at or below 0.1 M to prevent the solubilization of myosin within the tissue. After cryoprotection, the tissue was rapidly frozen in liquid nitrogen.

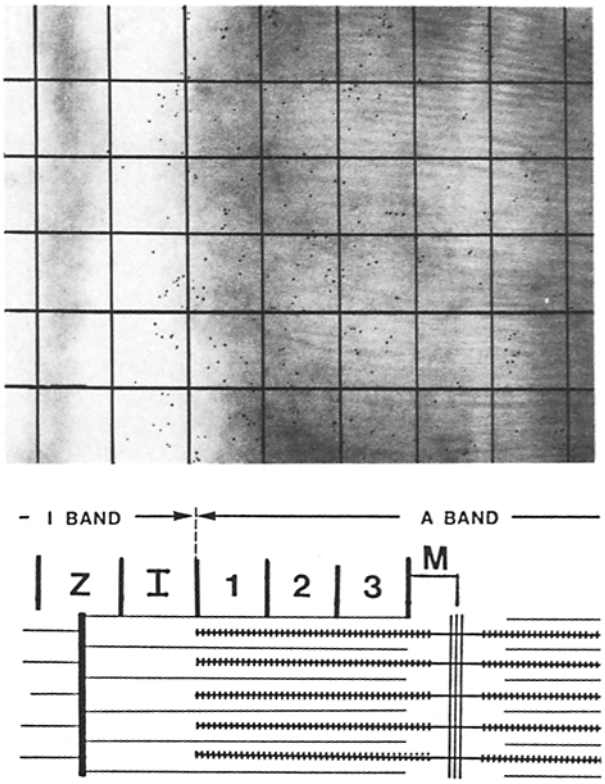

Figure 1. Electron micrograph of immunostained tissue is used for morphometric analysis. (*Top*) Test lattice is aligned with the sarcomere of the unfixed tissue from an animal treated with L-T3 for 3 d and immunostained with both mAb 37, anti-α-MHC, and GAr IgG gold. The lattice spacing of a square is 0.21 μm. (*Bottom*) Illustration of how the sarcomere is divided into bins for the determination of the distribution of the newly synthesized α-MHC.

Ultrathin (<0.1 μm) sections were cut on a cryosystem (NOVA; LKB Instruments, Inc., Gaithersburg, MD) at −110°C with a tungsten-coated glass knife (Roberts, 1975). Sections were retrieved with a drop of 2.3 M sucrose containing 0.75% gelatin (type III; Sigma Chemical Co.). The gelatin reduced the surface tension of the sucrose drop as it thawed, which decreased but did not eliminate fragmentation of the unfixed tissue.

Immunostaining

The tissue sections were preincubated with 1% BSA in 0.1 M PBS to block nonspecific binding of the antibodies and then sequentially incubated at room temperature on a rotating table with mAb 37 at a 1:100 dilution for 45 min and goat anti-rat (GAr) IgG-5-nm gold spheres (Janssen Life Sciences Products, Piscataway, NJ) at a 1:25 dilution for 45 min. All dilutions were made with 1% BSA in 0.1 M PBS. The sections were simultaneously stained and protected from drying artifact by 3% uranyl-acetate in 2% methyl cellulose. The tissue was viewed with a JEOL 100CX electron microscope at 100 kV.

The level of nonspecific binding of mAb 37 was determined on tissue from PTU hypothyroid animals, which has a very low content of α-MHC. To determine if the GAr IgG gold binds directly to the tissue without the presence of the primary antibody, 2-wk baby tissue, which has a high α-MHC content, was immunostained. Although the background binding of the GAr IgG gold was very low, it was not uniformly bound to all structural components. Therefore, paired tissue sections from each experimental animal were immunostained with only the GAr IgG gold to determine the relative level of nonspecific labeling of the various regions of the sarcomere.

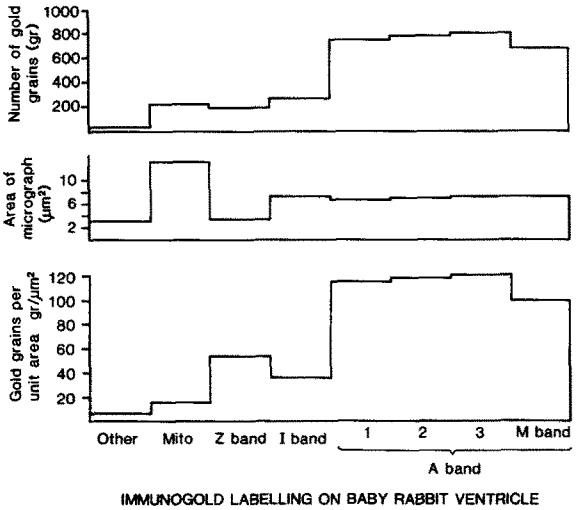

Figure 2. Immunolabeling of rabbit papillary muscle as a function of location within the sarcomere. Histograms of data from micrographs from 2-wk baby rabbit tissue sections immunostained with mAb 37, anti-α-MHC, and GAr IgG gold. (*Top*) Histogram of the number of gold grains counted for each designated region described in Fig. 1: A band, subdivided into four regions: 1, 2, 3, and M; I band; Z band; mitochondria (*Mito*); and intracellular regions not included in preceding categories (*Other*). (*Center*) Total area of tissue sampled for each designated region (μm^2). (*Bottom*) Raw gold density of each sarcomere division ($gr/\mu m^2$) has not been corrected for nonspecific staining of GAr IgG gold.

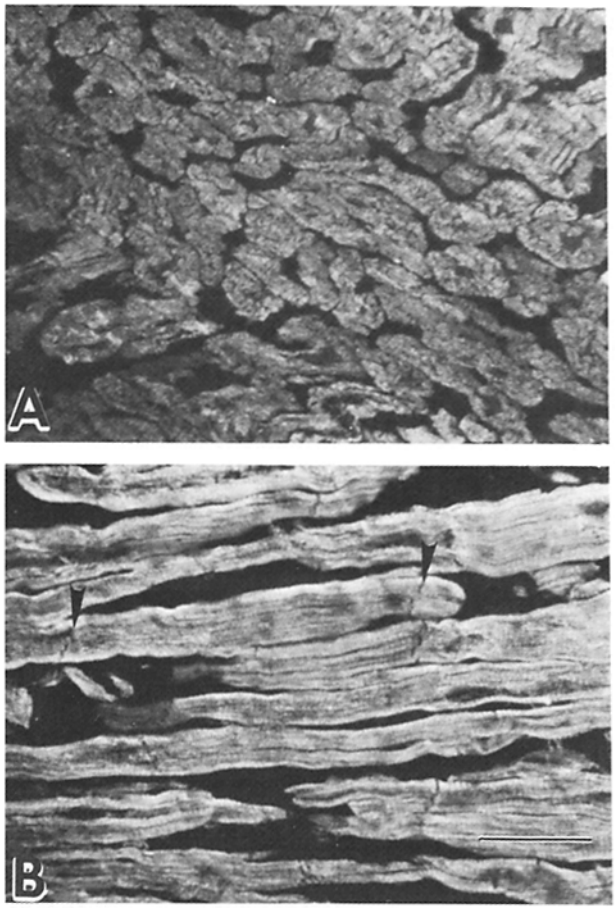

Figure 3. Uniform α-MHC distribution within the myocyte as detected by indirect immunofluorescence. (*A*) The papillary muscle of the left ventricle of a rabbit treated with L-T3 for 2 d and cut in cross section shows a homogeneous distribution of fluorescent signal across the diameter of individual myocytes. (*B*) Papillary muscle of a rabbit treated with L-T3 for 4 d cut in longitudinal section. Note the striated appearance due to A band staining and the even distribution of fluorescence throughout the length and the width of the cells. Arrows indicate intercalated disks. Bar, 50 μm.

Morphometric Analysis

A systematic sample was collected using only micrographs of longitudinally oriented sarcomeres in a noncontracted state. A minimum of nine micrographs of each tissue incubated in both mAb 37 and GAr IgG gold that contained sufficient area to yield over 1,000 grains were counted. A comparable total area was sampled from the paired section incubated only in the GAr IgG gold and yielded a low gold density.

The following classification system for the various regions of the sarcomere was used. The smallest repeating unit of the muscle, a half sarcomere, was divided into Z band, I band, and A band, which was further divided into four equally sized bins: 1, 2, 3, and M region (Fig. 1, bottom). The test lattice was placed over each micrograph to correspond with the sarcomere divisions (Fig. 1, top). At the print magnification of 48,000 used, each square of test lattice represented 0.044 μm^2. The total area was calculated by counting the number of squares corresponding to each region of the sarcomere (Weibel, 1979). The gold grains in each region were recorded and the gold densities in grains per square micrometer ($gr/\mu m^2$) were calculated for each region of the sarcomere and are shown as a histogram (Fig. 2).

The relative level of nonspecific labeling of the GAr gold to the various regions of the sarcomere was determined by comparing the average gold densities for each region from the paired tissue sections.

Results

Thyroid Model

The effectiveness of the thyroid hormone treatment in inducing a state of hyperthyroidism in the rabbits was assessed by a decrease in body weight and by an increase of the heart weight to body weight ratio for the adult animals (Sharp et al., 1985). The average weight of the animals at the beginning of the thyroid treatment was 3.1 ± 0.1 kg. The degree of weight loss in the experimental animals was related to the length of the thyroid treatment; 1- and 2-d animals lost 70 ± 40 g (n = 3 animals; mean ± SE), while 3- and 4-d animals lost 630 ± 80 g (n = 4 animals). The heart to body weight ratios were lowest in animals injected with thyroid for 1–2 d, 1.4 ± 0.14 (n = 3); while the ratio for 3- and 4-d injected animals (1.8 ± 0.09, n = 4) was greater than the ratio found in PTU animals (1.6 ± 0.02, n = 2), but less than the value obtained for normal erthyroid animals (2.3 ± 0.03, n = 2).

Immunofluorescence

Results from the indirect immunofluorescent experiments show a homogeneous distribution of fluorescent signal throughout the population of myocytes of the left ventricle and papillary muscle. Therefore, the thyroid dose was sufficient to upregulate expression of α-MHC in all myocytes by a similar amount and any section of tissue would thus be equally representative. The fluorescent signal is also homogeneously distributed within individual myocytes from 1–4-d thyroid-treated animals as illustrated with tissue in cross section from a 2-d animal and tissue in longitudinal section from a 4-d animal (Fig. 3, *A* and *B*, respectively).

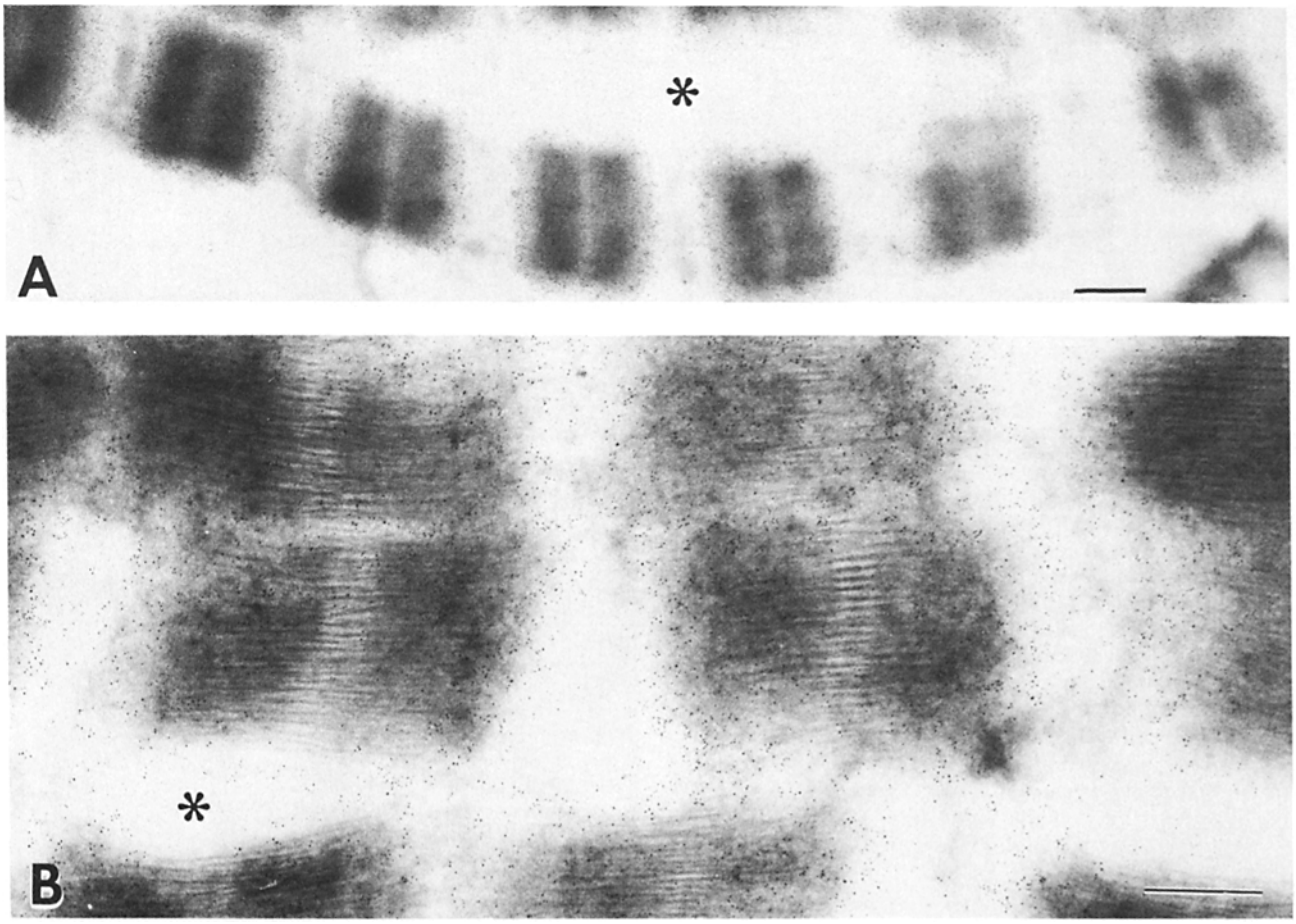

Figure 4. Immunoelectron micrograph of unfixed papillary muscle. Tissue is sampled from 4-d thyroid-injected animal, immunostained with mAb 37, anti-α-MHC, and GAr IgG gold. (*A*) Micrograph illustrates the fragmentation of the unfixed tissue incurred during the retrieval step of the ultracryomicrotomy. (*B*) Micrograph illustrates that the ultrastructure of the unfixed muscle is maintained during cryoprotection. Asterisks denote regions where fragmentation of the tissue is evident. Bars: (*A*) 1 μm; (*B*) 0.5 μm.

Ultracryomicrotomy and Immunostaining

Even without the benefit of fixation, myofibrillar structures maintained their integrity and ultrastructural detail (Fig. 4 *B*). In the unfixed tissue the spreading artifact was not completely prevented, even though gelatin was added to the sucrose drop used to retrieve the sections (Fig. 4 *A*). The level of nonspecific labeling of the GAr IgG gold on the thick filaments of the PTU-treated rabbits (Fig. 5 *A*) is very low (7 ± 2 gr/μm², n = 8, mean ± SE). As expected, the level of nonspecific labeling is greater when both antibodies are present (22 ± 3 gr/μm², n = 8) however, this gold density is very low. This indicates there is minimal nonspecific binding of the primary antibody, mAb 37 (Fig. 5 *B*).

The nonspecific labeling of the secondary antibody, GAr IgG gold, was determined on tissue sections from 2-wk-old baby rabbit heart (Fig. 6). Tissue incubated in both antibodies has a very high gold density in the A band (239 ± 54 gr/μm², n = 8) while the paired tissue sections incubated only in GAr IgG gold have a very low gold density (12 ± 1 gr/μm², n = 8). Therefore, nonspecific labeling of the α-MHC antigenic site by the secondary antibody, GAr IgG gold, is minimal.

The nonspecific binding of the immunoglobulins to the sarcomere is not the same in all regions of the sarcomere. The gold densities from the paired tissue sections incubated only in GAr IgG gold showed that the values for the Z band were twice as high (18.6 ± 5.4 gr/μm², n = 14) as any other bin (7.5 ± 2.2 gr/μm² of I band, n = 14; 9.3 ± 0.5 gr/μm² of A band bin, n = 14). As the Z band is known not to contain myosin, the Z band gold density was used as an internal standard in all samples to correct for nonspecific binding of the primary antibody. An example of the level of nonspecific labeling of the GAr IgG gold obtained in these experiments is seen in Fig. 7. This figure shows the gold density obtained when the tissue was exposed to only the GAr IgG gold (*solid bars*) or to both antimyosin, mAb 37, and GAr IgG gold (*open bars*) for each of the bins within the sarcomere. Corrections were made by subtraction of half of the Z band density from the raw gold densities of the A band of that same tissue section.

The corrected gold densities for the experimental animals showed the expected increases as a function of days of thyroid treatment. Furthermore, the nascent α-MHC is incorporated throughout the length of the thick filament with the average gold density per A Band bin increasing from 38 ± 6 gr/μm² (n = 8) in the 1-d treated animals to 182 ± 60 gr/μm² (n = 8) in the 4-d treated animal. Thus the average increase of α-MHC content detected by immunogold corre-

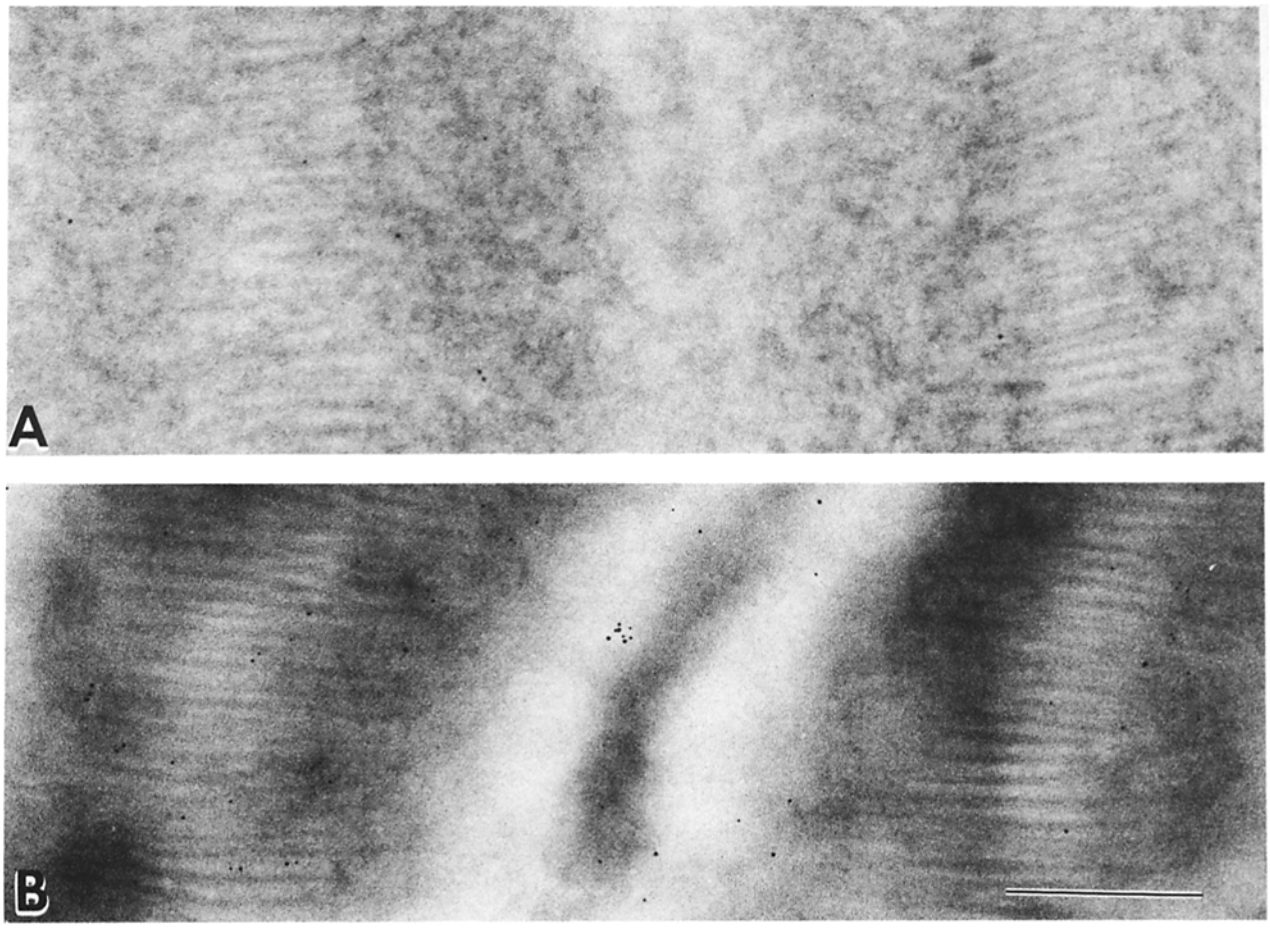

Figure 5. The level of nonspecific labeling of mAb 37, anti-α-MHC, was determined from electron micrographs of tissue from PTU-treated animals. (*A*) Tissue incubated with only GAr IgG gold has a low gold density. (*B*) Tissue incubated with both anti-α-MHC and GAr IgG gold also has a low gold density throughout the entire sarcomere. This indicates that the nonspecific labeling by the primary antibody, mAb 37 (anti-α-MHC) is minimal. Bar, 0.5 μm.

lates with the accumulation of α-MHC found by our immunofluorescent technique and with results from pyrophosphate gels (Chizzonite et al., 1982).

There is a uniform distribution of α-MHC within the first three bins (1, 2, and 3) of the thick filament in the myocytes of the 2-wk baby as seen in Fig. 2 (bottom). As mAb 37 binds to the hinge region of the myosin molecule, a lower gold density is expected in the center (region M) where the myosin rods are oriented in an antiparallel array, thereby affording fewer antigenic sites per length of filament. A similar uniform distribution pattern is seen in tissue from the normal animals and the PTU animals (Fig. 9). Therefore, the α-MHC antigen is equally accessible to the mAb 37 throughout the length of a thick filament and any nonuniformity of gold label must be attributable to a change in α-MHC distribution.

These experiments were designed to test the pattern of incorporation of nascent α-MHC into the thick filament. A pattern of A band labeling similar to that obtained in the control tissue (see Fig. 9) would indicate that newly synthesized α-MHC could exchange equally well with existing β-MHC throughout the length of the thick filament. The electron micrographs of typical sarcomeres (Fig. 8) give the impression that a gradient exists from the I band towards the M band. The quantitative data confirms this observation. Despite the average increase of gold density with days of thyroid treatment, the end of the thick filament (bin 1) always has a greater gold density than the center of the filament (bin M). The absolute gold densities are plotted as a function of location along the length of the A band in Fig. 9 and the morphometric analysis clearly shows a nonuniform pattern. There is a greater incorporation of the nascent myosin at the end than at the center of the A band. This is most evident in the 4-d thyroid-treated animal, but is also apparent to a lesser degree at earlier times.

The data was also analyzed on a relative basis; i.e., for every animal each region within the A band was calculated as a ratio of gold density of the bin to the average A band gold density. This method will tend to diminish the systematic errors inherent in immunostaining techniques. Tissue from normal and 2-wk baby animals was used as the control and has a uniform distribution of gold density along the A band, while the thyroid-treated animals show an increased gold density above the average at the ends of the thick filament (Fig. 10). In the thyroid-treated animals the distribution was not uniform, as the gold density in bin 1 was more than 50% greater than the average value, and, correspondingly, the M

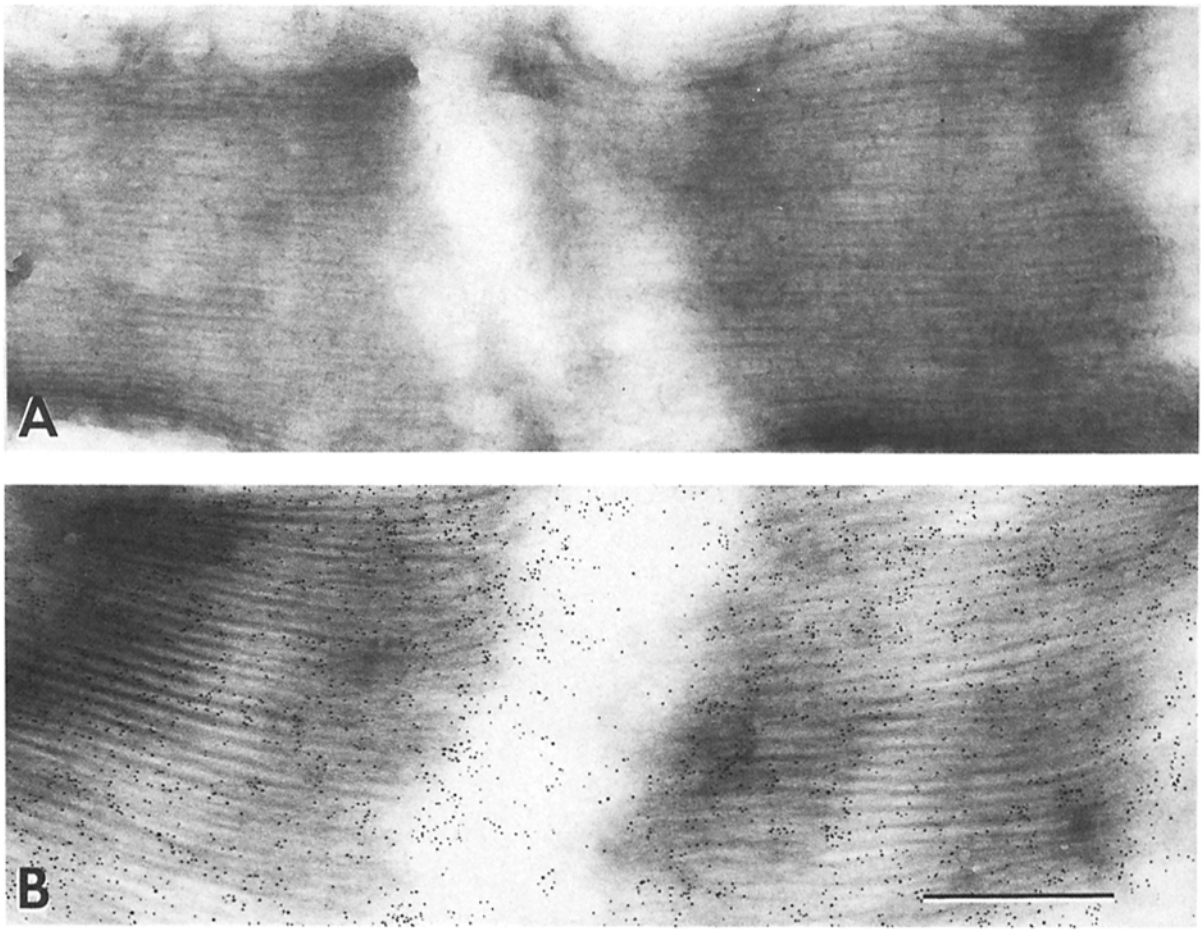

Figure 6. The level of nonspecific staining of the GAr IgG gold was determined from electron micrographs of tissue from 2-wk baby animals. (*A*) Tissue immunostained with only GAr IgG gold. The sparse gold labeling of this tissue indicates a low level of nonspecific labeling of the secondary antibody, GAr IgG gold. (*B*) Tissue immunostained with both mAb 37, anti-α-MHC, and GAr IgG gold. Note the dense gold labeling found throughout the A band and in the area of the I band. The high gold density is expected as 2-wk baby rabbit heart has a high content of α-MHC. Bar, 0.5 μm.

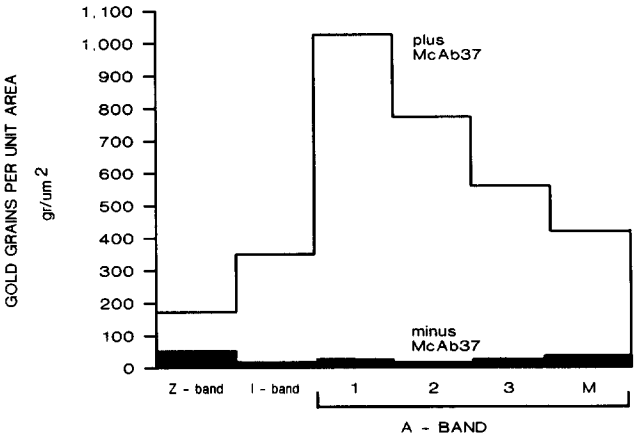

Figure 7. A histogram of the gold densities expressed as a function of location within the sarcomere of an animal treated with L-T3 for 4 d. Gold densities (gr/μm²) for each region of the sarcomere (see Fig. 1) were calculated from 10 micrographs. Tissue was either incubated in both anti-α-MHC, mAb 37, and GAr IgG gold (*open bars*) or only GAr IgG gold (*solid bars*). Note that though the level of nonspecific binding of the GAr IgG gold (*solid bars*) is low it is not uniform throughout the sarcomere as the Z band gold density is about twice as high as the other bins.

bin was 40% lower than the average (n = 7 animals). The conclusion again is a preferential addition of the α-MHC at the ends of the thick filaments.

An unexpected finding was the high density of gold grains found in the I band of two of the animals: one an experimental, the 4-d injected animal (Fig. 8 *D*), and one a control, the 2-wk baby rabbit (Fig. 6 *B*). It is unclear what mAb 37 is binding to in this area of the sarcomere.

Discussion

By manipulating the expression of cardiac myosin genes with thyroid hormone it was possible to follow the incorporation

Figure 8. Immunoelectron micrographs of sarcomeres from animals injected with thyroid hormone (L-T3) for 1, 2, 3, and 4 d (*A–D*, respectively). Tissue has been treated with mAb 37, anti-α-MHC, and GAr IgG gold. The gold label is mainly found in the A band and increases in density with the number of days of treatment. 1, 2, 3, and M refer to subdivisions of the A band as noted at bottom of Fig. 1. I band labeling is noted in the 4-d animal, see text for discussion. Bar, 0.5 μm.

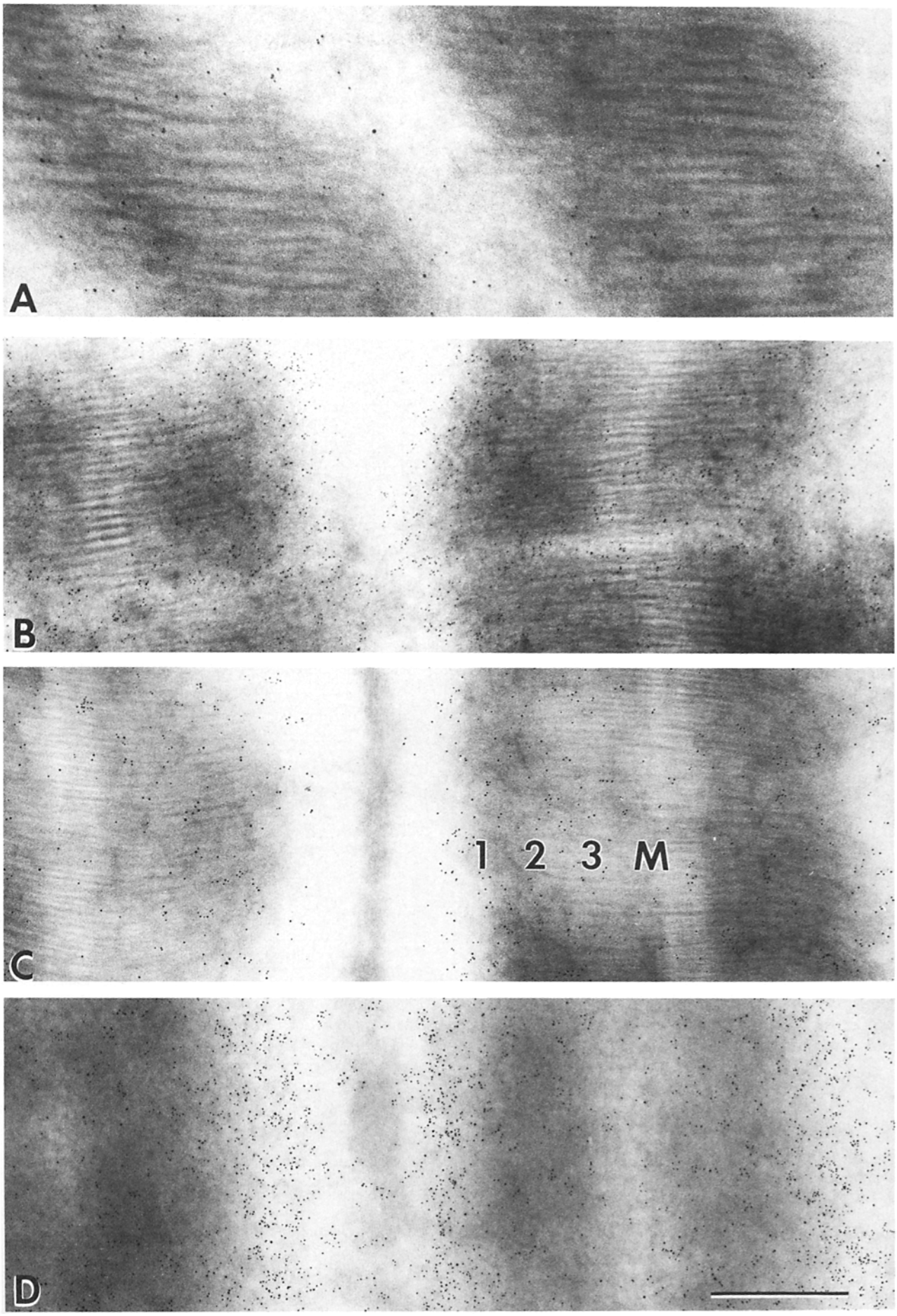
A
B
1 2 3 M
C
D

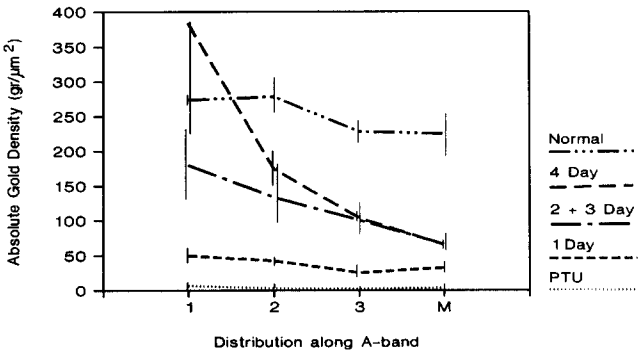

Figure 9. Absolute gold density (gr/μm²) of tissue from experimental animals as a function of location along the A band. Values have been corrected for nonspecific labeling of the antibodies by subtracting half the Z band gold density from each bin density (mean ± SE; $n = 2$ for all points except 2- and 3-d, where $n = 3$ animals; a minimum of nine micrographs for each animal was counted). The absolute gold density increases with days of thyroid treatment and there is a more rapid increase of nascent α-MHC at the ends of the A band (bin 1) than in the middle (bins 3 and M).

of new isomyosin into the myofibril in vivo. In the hyperthyroid model new myosin incorporates along the entire length of the thick filament with a preferential addition of the nascent α-MHC at the ends of the filament.

The technique of ultracryomicrotomy was essential to this experimental model to ensure that the observed pattern of gold labeling was not an artifact due to diffusion limitations of the immunoglobulins into the tissue sections. Access to the antigenic site could be limiting in either of the alternative techniques of pre- or postembedment immunostaining. During preembedment staining the immunoglobulin molecule must diffuse into a glycerinated myofibril structure (40 nm between thick filaments), while in postembedment staining the access to the tissue is limited by the matrix of the embedding medium. The nearly uniform distribution of gold density along the thick filament in controls, normal and 2-wk

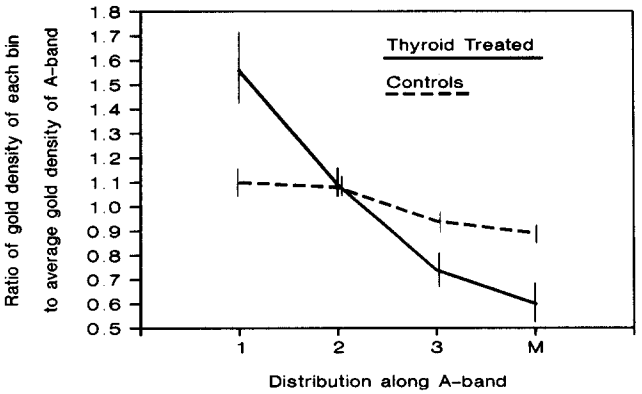

Figure 10. Gold density for each region of the A band is shown as a ratio of the gold density of the bin to the average gold density for the A band. The mean values and standard errors for animals treated with thyroid hormone ($n = 7$ animals), and for control animals, normal euthyroid and 2-wk-old baby ($n = 4$ animals). Note that there is a greater gold density at the end (bin 1) than at the center (bins 3 and M) of the thick filament.

baby (Fig. 8) obtained in our experiment indicates that accessibility to antigenic sites is not a function of location along the thick filament. One limitation of the immunocytochemical technique arises from the fact that antigenicity of the tissue is lost with each of the numerous fixations tried. All incubation solutions were kept at low ionic strength in order to limit the redistribution of myosin known to occur due to solubilization of myosin at high ionic strength. Redistribution of myosin due to exchange mechanisms can not be eliminated as it is only blocked by fixation (Saad et al., 1986*b*).

Studying the pattern of myosin exchange in thick filaments in vivo rather than in vitro indicates the possible effect of two major components of the sarcomere, myosin-associated proteins and the thin filament, on the myosin turnover process. Though numerous myosin-associated proteins have been identified (C, H, X, M protein, and titin [Offer et al., 1973; Starr et al., 1985; Eppenberger, 1981; Maruyama et al., 1977; Wang and Ramirez-Mitchell, 1983]), surprisingly little is known about their function. It is of interest that the C zone of the A band (Sjöström et al., 1977), which contains the C protein, corresponds with those bins (3 and M) that show the lowest gold densities in the thyroid-treated animals. When the integrity of titin is altered by either stretching the sarcomere beyond overlap or by subjecting the fiber to glycerination and calcium depletion, the thick filament does not reform during thick filament reconstitution experiments (Maw and Rowe, 1986). These results suggest that myosin-associated proteins may assist in maintaining thick filament integrity and may be involved in regulation of myosin turnover.

Myosin interaction with the thin filament appears to play a critical role in both assembly and stability of the thick filament structure. Results from thick filament reconstitution experiments (Maw and Rowe, 1986) suggest that thin filaments may play a major role in the concentration of myosin in the appropriate area of the sarcomere so as to enhance thick filament assembly and alignment with the thin filament, in effect, acting as a template for the thick filament formation. The process of myosin cross-bridge interaction with actin seems to stabilize the myofibrillar structure of contracting myocytes in culture, which have more myofibrils than noncontracting myocytes (Crisona and Strohmann, 1983). Given these findings it seemed essential to maintain the cross-bridge cycling function in a model of the myosin turnover phenomena.

Most in vitro thick filament assembly models work on isolated myosin preparations exclusive of associated proteins. Although this omission limits the extent to which the findings are applicable to the in vitro condition, they nonetheless provide important facts concerning thick filament assembly and disassembly. Some myosin types (i.e., skeletal, smooth, platelet myosin) are capable of forming synthetic hybrid filaments (Wachsberger and Pepe, 1980; Pollard, 1975) while others (brain myosin and myosin from *Physarium*) are not (Kuczmarski and Rosenbaum, 1979; Nachmias, 1972), which implies that the structural aspects of myosin that govern self-assembly show only a small degree of myosin-type specificity. Furthermore, the different myosin types appear to be uniformly distributed throughout the hybrid filament. This is in contrast to the situation found in nematode body wall musculature. Nematode thick filaments are composed of two myosin isoforms, A and B, which are segregated to the center and ends of the thick filament, respectively (Epstein et al.,

1982). The presence of more than one myosin isoform within an individual skeletal muscle fiber (Gauthier and Lowey, 1979) and within a cardiac myocyte (Samuel et al., 1983) has been detected using immunofluorescent techniques and is now an established phenomenon.

Saad et al. (1986*a*, *c*), using a fluorescence energy transfer system assay on synthetic thick filaments, have shown that myosin exchange can occur between thick filaments and is very rapid. This agrees with our result of a homogeneous distribution of the new myosin throughout the myocyte as seen at the light microscope level with indirect immunofluorescence. Over the course of the 24–96 h thyroid treatment period the new myosin is incorporated and exchanged between thick filaments, thereby presenting an appearance of uniform distribution throughout the myocytes. However, the increased accumulation at the ends of the thick filament seen with immunoelectron microscopy suggests that conditions found in vivo can prevent a homogenous distribution of the new myosin at the level of the thick filament.

The incorporation pattern of new myosin along the entire length of the thick filament is quite different from the minimal exchange of actin subunits found along the length of the thin filaments of rabbit skeletal muscle (Pardee et al., 1982). This is in contrast with the situation found in stress fibers of fibroblasts where actin incorporates throughout but has domains of slower incorporation due to the presence of actin-binding proteins (Amato and Taylor, 1986). The ability to incorporate anywhere in a filament allows for constant remodelling. Thus the pattern of myosin turnover, which allows exchange of myosin throughout the length of the thick filament, permits uninterrupted mechanical output during isoform exchange. Removal of a complete sarcomere would be detrimental to force transmission to adjacent units in series. Replacement of myosin all along the filament would be mechanically advantageous; large molecules can diffuse readily through contracting muscle (Barbosa and Da Silva, 1986).

Although with time all myosin will exchange along the thick filament, initially there is a preferential addition of the α-MHC at the ends of the thick filament. This pattern of incorporation could be a function of the increased protein synthesis rate seen with thyroid injection. During this state of rapid growth the rates of synthesis of α-MHC may be greater than the rates of incorporation of α-MHC into the thick filament. This imbalance would cause an accumulation of myosin at the rate limiting step in the assembly process. One kinetic model of assembly predicts that exchange between free myosin and the thick filament would occur more frequently at the ends of the thick filament with a lower rate of exchange occurring at the center of the thick filament. This model proposes that the length regulation in thick filaments is a function of a cumulative strain mechanism and that as the filament grows longer the dissociation constant increases exponentially (Davis, 1986). Rates of disassembly of the thick filament show a similar topological pattern (Ishiwata et al., 1985).

It has been shown that actin stress fiber–like structures play a major role in directing myofibrillogenesis in cultured chick cardiac myocytes (Dlugosz et al., 1984). Work by Maw and Rowe (1985) on thick filament reconstitution in myofibrils suggests that the thin filament acts as a scaffolding template for thick filament assembly. The greatest incorporation of α-MHC would therefore be expected in the overlap between A and I bands corresponding to bin 1 of the A Band. This is the region of the A band that shows the greatest percentage of α-MHC incorporation in our results (Figs. 8–10).

It is also of interest to note that in growing myocytes ribosomes are located between thick filaments but excluded from the M band (Larson et al., 1973). This region corresponds to bins 1–3 of the A band in our model. The thyroid treatment is known to up-regulate both α-MHC mRNA and rRNA (Everett et al., 1984). There is some evidence that implies translation of mRNA by the ribosome occurs in close proximity to the cellular location of that particular protein. For example, in fibroblasts, the mRNA for actin is localized near sites of actin accumulation (Lawrence and Singer, 1986).

An increased gold density in the I band was noted in two of the animal groups, the 2-wk baby and the 4-d injected animal. Any imbalance between the processes of protein synthesis and protein incorporation would be most evident in these two groups, as they are expected to have the most rapid growth rates. Though the I band is by definition that region of the sarcomere that does not contain thick filaments, it nevertheless does have as a major component titin (Wang and Ramirez-Mitchell, 1983; Maruyama et al., 1985*a*), which is known to bind the light meromyosin portion of myosin (Maruyama et al., 1985*b*). More recent work by Isaacs and Fulton (1986) has shown that nascent MHC are associated with the actin filaments of the cytoskeleton in developing chick skeletal muscle. Therefore, the nascent myosin made during the hyperthyroid period may be interacting with the proteins located in the I band. Of course the distribution of α-MHC along the thick filament in the 2-wk baby is not expected to show the preferential accumulation of α-MHC at the ends of the A band because the primary antibody, mAb 37, is unable to distinguish the nascent α-MHC from the α-MHC that is already present at high levels in the 2-wk-old baby rabbit. Furthermore, we would predict that a homogeneous distribution of α-MHC along the A band would be present in long-term hyperthyroid animals.

The results from this experiment support the hypothesis of myosin turnover throughout the length of the thick filament in a nonsegregated manner. However, during periods of high rates of protein synthesis another aspect of the turnover process becomes evident. This involves a possible imbalance between the rates of synthesis and incorporation that results in accumulation of new myosin at the ends of the thick filament. This imbalance is a result of a factor(s) that is associated with conditions found in intact functioning myocytes.

We thank Dr. R. Zak for the monoclonal antibody 37.

Research was supported by grants from the American Heart Association and from the National Institutes of Health (HL 35728). M. P. Wenderoth was supported in part by a National Research Service Award from the National Institute of Health (HL 07320).

Received for publication 18 May 1987, and in revised form 4 August 1987.

References

Amato, P. A., and D. L. Taylor. 1986. Probing the mechanism of incorporation of fluorescently labeled actin into stress fibers. *J. Cell Biol.* 102:1074–1084.

Barbosa, M. L., and P. P. Da Silva. 1986. Ultrastructural patterns of ferritin permeation into glutaraldehyde-fixed freeze-fractured sarcomeres characterize stages of contraction in striated muscle. *J. Electron Microsc.* 4:329–342.

Chizzonite, R. A., A. W. Everett, W. A. Clark, S. Jakovcic, M. Rabinowitz, and R. Zak. 1982. Isolation and characterization of two molecular variants

of myosin heavy chain from rabbit ventricle. *J. Biol. Chem.* 257:2056–2060.
Crisona, N. J., and R. C. Strohman. 1983. Inhibition of contraction of cultured muscle fibers results in increased turnover of myofibrillar proteins but not of intermediate-filament proteins. *J. Cell Biol.* 96:684–692.
Davis, J. S. 1986. A model for length-regulation in thick filaments of vertebrate skeletal myosin. *Biophys. J.* 50:417–422.
Dlugosz, A. A., P. B. Antin, V. T. Nachmias, and H. Holtzer. 1984. The relationship between stress fiber-like structures and nascent myofibrils in cultured cardiac myocytes. *J. Cell Biol.* 99:2268–2278.
Eisenberg, B. R., J. A. Edwards, and R. Zak. 1985. Transmural distribution of isomyosin in rabbit ventricle during maturation examined by immunofluorescence and staining for calcium-activated adenosine triphosphate. *Circ. Res.* 56:548–555.
Eppenberger, H. M., J. C. Perriard, U. B. Rosenberg, and E. E. Strehler. 1981. The M_r 165,000 M-protein myomesin: a specific protein of cross-striated muscle cells. *J. Cell Biol.* 89:189–193.
Epstein, H. F., S. A. Berman, and D. M. Miller III. 1982. Myosin synthesis and assembly in nematode body-wall muscle. *In* Muscle Development: Molecular and Cellular Control. M. L. Pearson and H. F. Epstein, editors. Cold Spring Harbor Laboratory, Cold Spring Harbor, NY. 419–427.
Everett, A. W., A. Sinha, P. K. Umeda, S. Jakovcic, M. Rabinowitz, and R. Zak. 1984. Regulation of myosin synthesis by thyroid hormone: relative change in the alpha and beta-myosin heavy chain mRNA levels in rabbit heart. *Biochemistry.* 23:1596–1599.
Gauthier, G. F., and S. Lowey. 1979. Distribution of myosin isoenzymes among skeletal muscle fiber types. *J. Cell Biol.* 81:10–25.
Harrington, W. F., and M. E. Rodgers. 1984. Myosin. *Annu. Rev. Biochem.* 53:35–73.
Higuchi, H., and S. Ishiwata. 1985. Disassembly kinetics of thick filaments in rabbit skeletal muscle fibers: effect of ionic strength, Ca2+ concentration, pH, temperature, and cross-bridges on the stability of thick filament structure. *Biophys. J.* 47:267–275.
Hoh, J. F., P. A. McGrath, and P. T. Hale. 1978. Electrophoretic analysis of multiple forms of cardiac myosin: effect of hypophysectomy and thyroxine replacement. *J. Mol. Cell. Cardiol.* 10:1053–1076.
Huxley, H. E. 1963. Electron microscope studies on the structure of natural and synthetic protein filaments from striated muscle. *J. Mol. Biol.* 7:281–308.
Isaacs, W. B., and A. B. Fulton. 1987. Cotranslational assembly of myosin heavy chain in developing cultured skeletal muscle. *Proc. Natl. Acad. Sci. USA.* 84:6174–6178.
Ishiwata, S., K. Muramatsu, and H. Higuchi. 1985. Disassembly from both ends of thick filaments in rabbit skeletal muscle fibers. *Biophys. J.* 47: 257–266.
Kovacs, L., E. Rios, and M. F. Schneider. 1983. Measurement and modification of free calcium transients in frog skeletal muscle fibres by metallochromic indicator dye. *J. Physiol. (Lond.).* 343:161–196.
Kuettel, M. R., S. P. Squinto, J. Kwast-Welfeld, G. Schwoch, J. S. Schweppe, and R. A. Jungmann. 1985. Localization of nuclear subunits of cyclic AMP-dependent protein kinase by the immunocolloidal gold method. *J. Cell Biol.* 101:965–975.
Kuczmarski, E. R., and J. L. Rosenbaum. 1979. Chick brain actin and myosin: Isolation and characterization. *J. Cell Biol.* 80:341–355.
Larson, P. F., J. J. Fulthorpe, and P. Hudgson. 1973. The alignment of polysomes along myosin filaments in developing myofibrils. *J. Anat.* 116:327–334.
Lawrence, J. B., and R. H. Singer. 1986. Intracellular localization of messenger RNAs for cytoskeletal proteins. *Cell.* 45:407–415.
Maruyama, K., S. Kimura, K. Wakabayashi, T. Yamamoto, and T. Suzuki. 1985*a*. Connectin causes aggregation of myosin rods but not of myosin heads. *Biomed. Res.* 6:423–427.
Maruyama, K., S. Matsubara, R. Natori, Y. Nonomura, S. Kimura, K. Ohashi, F. Murakami, and S. Handa. 1977. Connectin, an elastic protein of muscle. *J. Biochem. (Tokyo).* 82:317–337.
Maruyama, K., T. Yoshioka, H. Higuchi, K. Ohashi, S. Kimura, and R. Natori. 1985*b*. Connectin filaments link thick filaments and Z lines in frog skeletal muscle as revealed by immunoelectron microscopy. *J. Cell Biol.* 101:2167–2172.
Maw, M. C., and A. J. Rowe. 1986. The reconstruction of myosin filaments in rabbit psoas muscle from solubilized myosin. *J. Muscle Res. Cell Motil.* 7:97–109.
McLean, I. W., and P. K. Nakane. 1974. Periodate-lysine-paraformaldehyde fixative: a new fixative for immunoelectron microscopy. *J. Histochem. Cytochem.* 22:1077–1083.
Morkin, E., S. Kimata, and J. J. Skillman. 1972. Myosin synthesis and degradation during development of cardiac hypertrophy in the rabbit. *Circ. Res.* 30:690–702.
Nachmias, V. T. 1972. Filament formation by purified Physarium myosin. *Proc. Natl. Acad. Sci. USA.* 69:2011–2014.
Offer, G., C. Moos, and R. Starr. 1973. A new protein of the thick filament of vertebrate skeletal myofibrils: extraction, purification and characterization. *J. Mol. Biol.* 74:653–676.
Pardee, J. D., P. A. Simpson, L. Stryer, and J. A. Spudich. 1982. Actin filaments undergo limited subunit exchange in physiological salt conditions. *J. Cell Biol.* 94:316–324.
Pearse, A. G. E., and J. M. Polak. 1975. Bifunctional reagents as vapour- and liquid-phase fixatives for immunohistochemistry. *Histochem. J.* 7:179–186.
Pepe, F. A. 1983. Macromolecular assembly of myosin. *In* Muscle and Nonmuscle Motility. A. Stracher, editor. Academic Press, Inc., New York. 105–145.
Pollard, T. D. 1975. Electron microscopy of synthetic myosin filaments: evidence for cross-bridge flexibility and copolymer formation. *J. Cell Biol.* 67:93–104.
Reisler, E., P. Cheung, N. Borochov, and J. A. Lake. 1986. Monomers, dimers, and minifilaments of vertebrate skeletal myosin in the presence of sodium pyrophosphate. *Biochemistry.* 25:326–332.
Roberts, I. M. 1975. Tungsten coating: a method of improving glass microtome knives for cutting ultrathin frozen sections. *J. Microsc. (Oxf.).* 103:113–119.
Saad, A. D., D. A. Fischman, and J. D. Pardee. 1986*a*. Fluorescence energy transfer studies of myosin thick filament assembly. *Biophys. J.* 49:140–142.
Saad, A. D., K. A. Hamilton, and D. A. Fischman. 1986*b*. Effects of myosin concentration and cross-linking on exchange of myosin between thick filaments. *J. Cell Biol.* 103(5, Pt. 2):117a. (Abstr.)
Saad, A. D., J. D. Pardee, and D. A. Fischman. 1986*c*. Dynamic exchange of myosin molecules between thick filaments. *Proc. Natl. Acad. Sci. USA.* 83:9483–9487.
Samuel, J. L., L. Rappaport, J.-J. Mercadier, A.-M. Lompre, S. Sartore, C. Triban, S. Schiaffino, and K. Schwartz. 1983. Distribution of myosin isozymes within single cardiac cells, an immunohistochemical study. *Circ. Res.* 52:200–209.
Sharp, N. A., D. S. Neel, and R. L. Parsons. 1985. Influence of thyroid hormone levels on the electrical and mechanical properties of rabbit papillary muscle. *J. Mol. Cell Cardiol.* 17:119–132.
Sjöström, M., and J. M. Squire. 1977. Fine structure of the A-band in cryosections: the structure of the A-band of human skeletal muscle fibres from ultrathin cryo-sections negatively stained. *J. Mol. Biol.* 109:49–68.
Starr, R., R. Almond, and G. Offer. 1985. Location of C-protein, H-protein, and X-protein in rabbit skeletal muscle fibre types. *J. Muscle Res. Cell Motil.* 6:227–256.
Tokuyasu, K. T. 1986. Application of cryoultramicrotomy to immunocytochemistry. *J. Microsc. (Oxf.).* 143:139–149.
Tokuyasu, K. T., A. H. Dutton, B. Geiger, and S. J. Singer. 1981. Ultrastructure of chicken cardiac muscle as studied by double immunolabeling in electron microscopy. *Proc. Natl. Acad. Sci. USA.* 78:7619–7623.
Umeda, P. K., S. Jakovcic, and R. Zak. 1986. RNA transcription in heart muscle. *In* The Heart and Cardiovascular System. H. A. Fozzard, editor. Raven Press, New York. 949–963.
Wachsberger, P. R., and F. A. Pepe. 1980. Interaction between vertebrate skeletal and uterine muscle myosins and light meromyosins. *J. Cell Biol.* 85:33–41.
Wang, K., and R. Ramirez-Mitchell. 1983. A network of transverse and longitudinal intermediate filaments is associated with sarcomeres of adult vertebrate skeletal muscle. *J. Cell Biol.* 96:562–570.
Weibel, E. R. 1979. Practical methods for biological morphometry. *In* Stereological Methods. Vol. 1. Academic Press, Inc., New York. 415 pp.
Willingham, M. C., and S. S. Yamada. 1979. Development of a new primary fixative for electron microscopic immunocytochemical localization of intracellular antigens in cultured cells. *J. Histochem. Cytochem.* 27:947–960.
Zak, R., R. A. Chizzonite, A. W. Everett, and W. A. Clark. 1982. Study of ventricular isomyosins during normal and thyroid hormone induced cardiac growth. *J. Mol. Cell Cardiol.* 14(Suppl. 3):111–117.